EUROPEAN ORGANIZATION FOR NUCLEAR RESEARCH

July 24, 1997

Measurements of the Structure of Quark and Gluon Jets in Hadronic Z Decays

The ALEPH Collaboration

Abstract

In this paper, an experimental investigation of the structure of identified quark and gluon jets is presented. Observables related to both the global and internal structure of the jets are measured; this allows for tests of QCD over a range of transverse momentum scales. The observables include distributions of jet-shape variables, the mean and standard deviation of the subjet multiplicity distribution, and the fragmentation function for charged particles. The measurements are based on 3×10^6 hadronic Z decays recorded by the ALEPH detector at the LEP storage ring. From these, 70 000 nearly symmetric three-jet events are selected using the Durham clustering algorithm with a jet resolution parameter of $y_{\mathrm{cut}} = 0.1$. A gluon jet is identified by requiring evidence for long-lived heavy-flavour hadrons in the other two jets; this results in a sample of about 4000 gluon jets with a purity of 94.4%. The measurements are compared with the predictions of Monte Carlo models and recently calculated QCD predictions, which are now available for quark and gluon jets separately. The latter comparison shows that leading and next-to-leading logarithmic contributions are necessary to extend agreement to lower momentum-transfer scales.

(Submitted to the 1997 lepton-photon conference, Hamburg)

1 Introduction

In a previous publication by the ALEPH collaboration [1], "Mercedes star" like three-jet events were used to investigate the internal structure of identified quark and gluon jets. Since then, theoretical developments [2, 3] and the availability of additional data have motivated an update and extension of the analysis. The measurements are now repeated with a larger data sample and a more detailed study of systematic errors. In addition, new observables are investigated which allow for tests of QCD over a broad range of Q^2 scales.

The measurements are based on approximately 3×10^6 hadronic Z decays recorded by the ALEPH detector [4] at the LEP storage ring, operating at a centre-of-mass energy of $E_{cm} = 91.2$ GeV. From these, 70 000 three-jet events are selected using the Durham clustering algorithm [5] with a jet resolution parameter of $y_{\rm cut} = y_1 = 0.1$. A gluon jet is identified by requiring evidence for long-lived heavy-flavour hadrons in the other two jets; this results in a sample of 4000 gluon jets with a purity of 94.4%. By measuring the properties of all jets in the three-jet sample (consisting of 2/3 quark and 1/3 gluon jets) as well as in the gluon enriched sample, the properties of quark and gluon jets are inferred.

An important feature of the analysis is the choice of a relatively large resolution parameter ($y_1 = 0.1$) to select the three-jet events. This leads to well-separated jets, where the smallest interjet angle is typically greater than 90 degrees. In addition, it is possible to study the internal jet structure up to the scale of $y_1 = 0.1$; this extends well into the range where perturbative predictions are valid.

2 Definition of observables

Distributions of event-shape variables are well established as a useful measure of the global structure of hadronic final states. In analogy with these, distributions of jet-shape variables allow one to characterize the overall structure of quark and gluon jets. Corresponding to the variables wide and narrow jet broadening, defined for particles in separate hemispheres of an event [6], jet broadening is defined in this analysis for each jet as

$$B_{\rm jet} = \frac{\sum_{i=1}^{N} |p_\perp^i|}{\sum_{i=1}^{N} |p^i|},$$

where $p_\perp^i$ is the momentum of particle i transverse to the jet axis, and the sum extends over all of the N particles in the jet. This can be thought of as a measure of the transverse structure of a jet.

Another jet-shape variable called y_2 (also referred to as the differential one-subjet rate) is defined by clustering the particles in a jet until two clusters (subjets) result. The value of y_2 is then given by the Durham scale between the two subjets. The value of the distribution is directly related to the probability for a parton to split into two further partons which are resolved at a scale y_2.

For both $B_{\rm jet}$ and y_2, ranges of the distributions related to hard gluon emission can be identified. Here the influences of nonperturbative effects (hadronization) are small, and the predictions of perturbative QCD are expected to be reliable.

In order to investigate the internal jet structure, the particles of the individual jets are clustered using again the Durham clustering algorithm. Now, however, a subjet resolution scale y_0 less than y_1 is used, so that subjets are resolved. The mean values ($\langle N_{\rm g} - 1\rangle$, $\langle N_{\rm q} - 1\rangle$)

and standard deviations (σ_g, σ_q) of the subjet multiplicity distribution are then measured as a function of y_0. In addition, the ratios

$$R_N(y_0) = \frac{\langle N_g(y_0) - 1\rangle}{\langle N_q(y_0) - 1\rangle}\,, \qquad R_\sigma(y_0) = \frac{\sigma_g(y_0)}{\sigma_q(y_0)}\,,$$

are determined. By subtracting unity from $\langle N_g\rangle$ and $\langle N_q\rangle$, the observables are directly related to the probability for additional partons to be emitted from the original gluon or quark. In addition, this definition results in a simple expression for the perturbative prediction at leading-log accuracy for R_N of $C_A/C_F = 9/4$, valid for all values of y_0. For sufficiently large y_0, corresponding to a sufficiently large transverse momentum separation between subjets, one expects that perturbative predictions should be valid and that the subjets should thus reflect the underlying partonic structure of the event. By going to smaller values of y_0 one can investigate the extent to which the perturbative predictions remain valid and determine scales where non-perturbative effects become important.

The mean values $\langle N_g{-}1\rangle$ and $\langle N_q{-}1\rangle$ reported here represent updates of previously published values [1], here based on a larger data sample and with further studies of systematic uncertainties. The standard deviations σ_g and σ_q are measured here for the first time. The means and standard deviations are now also measured as a function of jet energy, opening a new degree of freedom for QCD tests.

In the limit of small subjet scales ($y_0 \to 0$), individual particles are resolved. From these, the distributions (fragmentation functions) of $x = E_{\mathrm{hadron}}/E_{\mathrm{jet}}$ have been measured for charged particles in quark and gluon jets. These can be used to predict quark and gluon fragmentation functions for other processes and at other energy scales.

3 Analysis procedure and systematic errors

The analysis procedure used is almost the same as the one described in the previous ALEPH publication on subjets [1]. For observables which are studied as a function of jet energy, however, the procedure is generalized; in particular, the gluon jet purities must be determined as a function of E_{jet}.

From the data sample available, 3 million hadronic Z decays are selected. By applying the Durham algorithm with a jet resolution parameter of $y_{\mathrm{cut}} = y_1 = 0.1$ and requiring a minimum angle of 35° between each jet and the beam axis, about 70 000 "Mercedes star" like three-jet events are selected. These correspond to Z decays into $q\bar{q}$ with the subsequent emission of a high energy gluon. From these, 4 000 gluon jet candidates are identified by applying a three dimensional impact parameter method for long-lived heavy-flavour hadrons [7]. By measuring the various observables for the gluon jet candidates and in addition for all of the jets in the three-jet sample (consisting of 1/3 gluon and 2/3 quark jets), the corresponding quantities for pure quark and gluon jets are determined.

Because of the larger data sample compared to that used in the previous ALEPH publication on subjets, possible sources of systematic uncertainties were investigated in greater detail. The following sources of uncertainty were found to be important. First, the correction factors derived from the Monte Carlo, which are used to correct the observables for detector effects, could have a dependence on the event generator used. This was investigated by computing simplified correction factors using the generators JETSET 7.4 [8], HERWIG 5.8 [9] and ARIADNE 4.06 [10], and including the maximum variation in the results in the systematic error. In addition, the accuracy of the detector simulation was investigated by successively varying the analysis cuts and repeating the analysis. The largest deviations in results from those based on standard cuts come from the following variations: (a) minimum energy required for neutral particles, (b) minimum angle required between jet axis and beam axis in order to measure the complete jet in the detector, (c) the selection cut for identifying gluon jet candidates.

The total systematic error is obtained by adding the four contributions above in quadrature. The relative sizes of these contributions differ from observable to observable and also vary over the measured range of a given observable. As a general rule, the total systematic error is comparable to the statistical error.

4 Results

In the following sections the measurements are presented and compared to analytic predictions of QCD and to predictions of Monte Carlo models. The important parameters of the models were tuned to describe ALEPH measurements of charged particle inclusive and event-shape distributions [11]. The error bars on the plots show the quadratic sum of statistical and systematic uncertainties.

4.1 Jet-shape variables

The measured $B_{\rm jet}$ distribution is shown in Fig. 1 along with the predictions of the Monte Carlo models JETSET, HERWIG and ARIADNE. In general, all of the models describe the data reasonably well, although the ARIADNE prediction for gluon jets is systematically shifted to too high values of $B_{\rm jet}$.

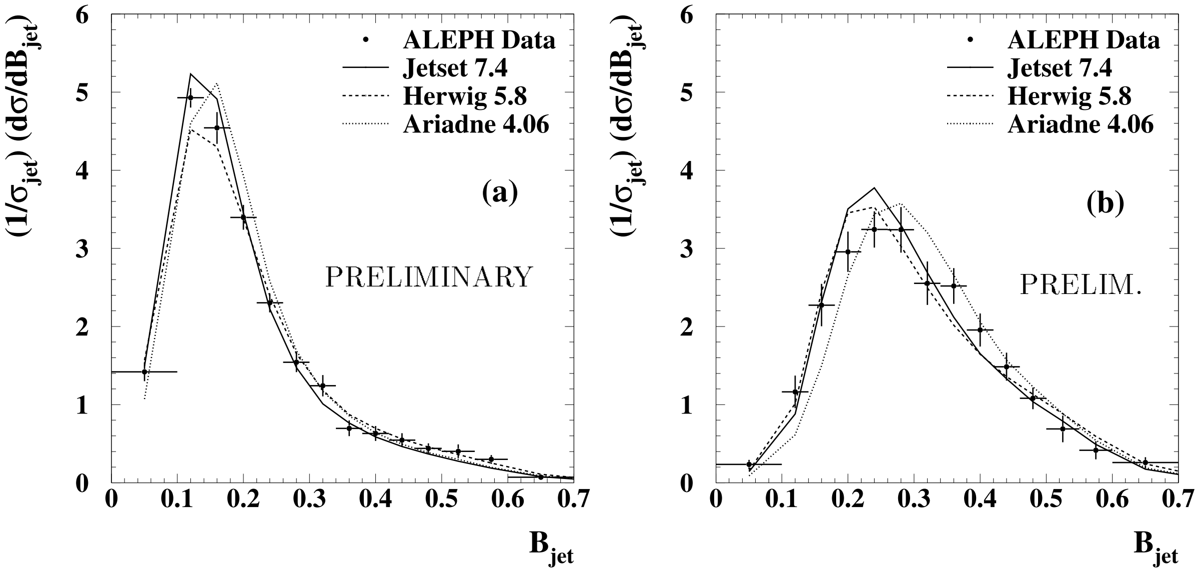

Figure 1: The measured $B_{\rm jet}$ distribution for (a) quark and (b) gluon jets in comparison with Monte Carlo models.

In particular, there is good agreement in the regions of large $B_{\rm jet}$, where hadronization corrections are small and the distributions are sensitive to perturbative physics. This was investigated with the JETSET model by comparing the B_{jet} distributions at parton and hadron level. As can be seen in Fig. 2(a), hadronization effects are negligible at large B_{jet}.

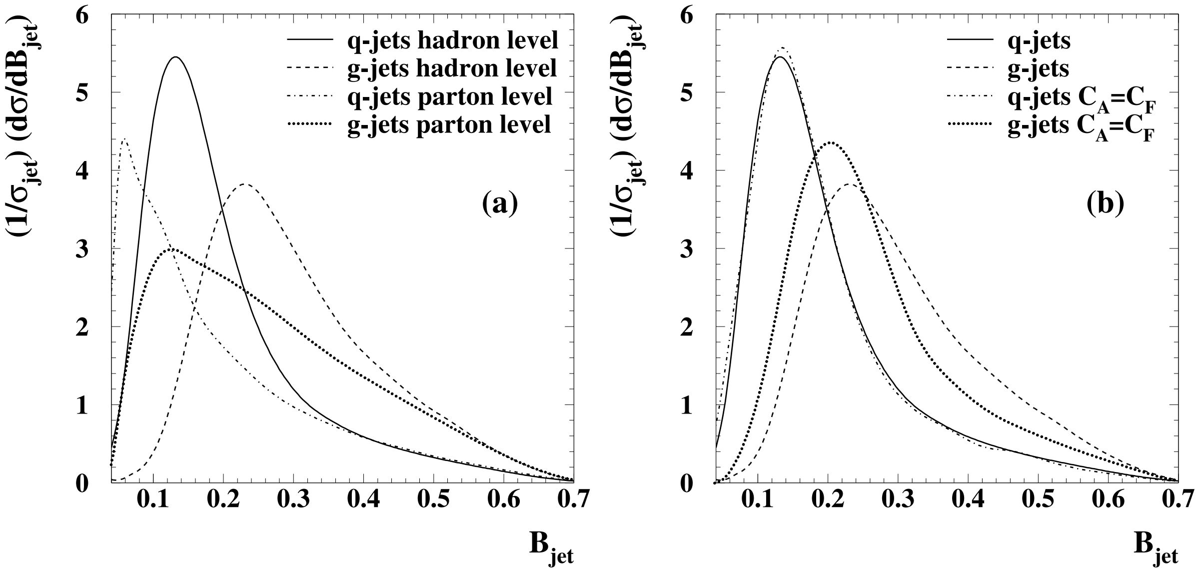

Figure 2: The B_{jet} distribution predicted by the JETSET 7.4 Monte Carlo (a) comparing hadron and parton level distributions, and (b) comparing hadron level distributions with different couplings for the parton splitting $g \to gg$ (see text).

In order to investigate whether the distribution is sensitive to perturbative physics, the effective coupling of the splitting $g \to gg$ was changed from its QCD value $C_A\alpha_S$ to $C_F\alpha_s$ (where $C_A = 3$ and $C_F = 4/3$), which is the corresponding value for $q \to qg$. The resulting hadron-level distributions are shown in Fig. 2(b). The quark-jet distribution remains largely unchanged, whereas the distribution for gluon jets is suppressed at large B_{jet}. A large part of the difference between quark and gluon jets is thus seen to stem from the higher effective colour charge of the gluon, rather than being, for example, a simple consequence of kinematics. Similar results are found for the y_2 distribution.

Figure 3 shows the measured y_2 distribution for quark and gluon jets along with the predictions of Monte Carlo models and also from leading order (LO) QCD [3] without any modifications for hadronization. The LO prediction is expected to be valid only in the region of large y_2 (small $L_2 = -\ln y_2$) where hard emission dominates and hence the effects of higher orders should be small. For small y_2 emission of soft and collinear partons becomes important. In fact, the prediction shows significant discrepancies with the data already for L_2 above 4 (y_2 below 0.018). Monte Carlo studies with the y_2 distribution lead to similar conclusions concerning sensitivity to hadronization and perturbative effects in the region of large y_2 as was seen for large B_{jet}.

4.2 Subjet structure without consideration of jet energy

First the properties of the subjet multiplicity distribution are examined without consideration of the jet energy. Various properties are shown as a function of the resolution parameter y_0 in Fig. 4 along with the predictions of the JETSET, HERWIG and ARIADNE models. Figures 4 (a) and (b) show the mean subjet multiplicity minus one for gluon and quark jets, and (c) shows their ratio R_N. The standard deviations σ_{g} and σ_{q} and their ratio R_σ are shown in Figs. 4 (d)

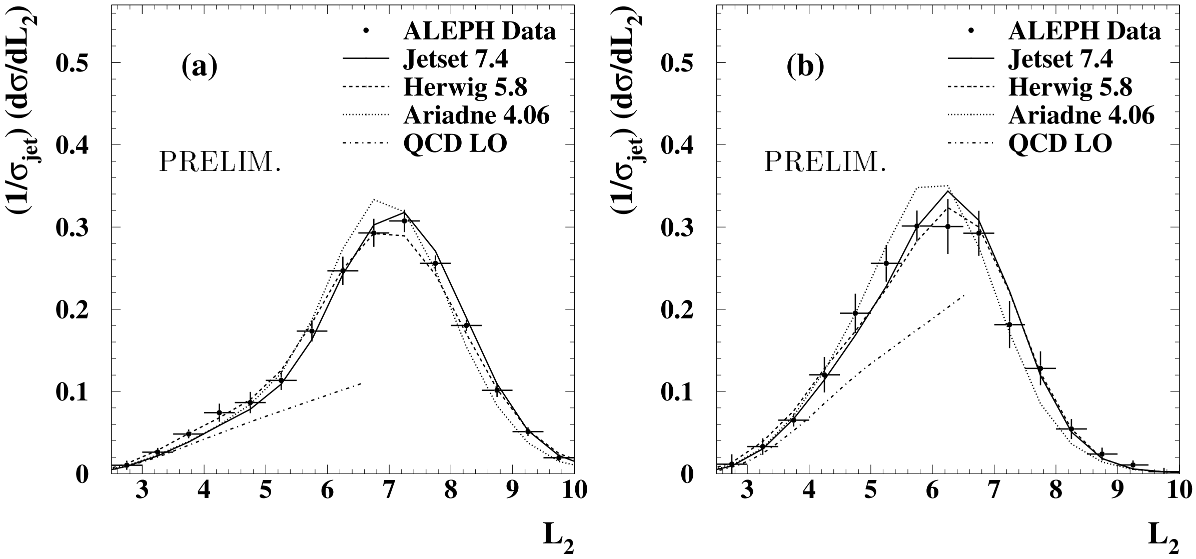

Figure 3: The measured $L_2 = -\ln y_2$ distribution for (a) quark and (b) gluon jets compared to the predictions of Monte Carlo models. The dashed-dotted curve shows the leading-order QCD prediction.

– (f).

The agreement with the Monte Carlo models is seen to be qualitatively very good, especially when one considers that the observables vary over several orders of magnitude within the range studied. For the mean subjet multiplicities, this confirms the observations in [1], now at a sufficiently high level of precision to discriminate between models. For the multiplicities $\langle N_{\rm g}-1\rangle$, $\langle N_{\rm q}-1\rangle$ and their ratio R_N, HERWIG is seen to give the best description. The predicted multiplicities from ARIADNE are significantly high for both quark and gluon jets, but there is better agreement for the ratio. It should be noted, however, that the relative size of the total errors is only around 1 – 2 % for $y_0 < 10^{-3}$ and that the results for neighbouring values of y_0 are highly correlated.

For the standard deviations and their ratio, the picture is somewhat different. There, all models provide a good description of the gluon jets. For the quark jets, however, HERWIG predicts a too broad subjet multiplicity distribution, especially at small y_0. This observation is of particular interest, since previous measurements had shown that HERWIG's prediction for the width of the charged particle multiplicity distribution for entire events was also significantly too large [11, 12]. This discrepancy is now seen to stem from the quark jets only.

In Fig. 5, the same results are compared with perturbative QCD predictions without any modifications for hadronization effects [2], as well as with the hadron- and parton-level predictions of the JETSET model. From the comparison of the hadron and parton levels of JETSET for the observables $\langle N_{\rm g}-1\rangle(y_0)$, $\langle N_{\rm q}-1\rangle(y_0)$, $\sigma_{\rm g}(y_0)$, and $\sigma_{\rm q}(y_0)$, one can see that the effects of hadronization are small as long as y_0 is sufficiently large. This range of y_0 values ($y_0 > 10^{-3}$) will be referred to as the perturbative region. For small y_0, however, hadronization effects continue to increase. But one should note that the parton level in the Monte Carlo model is not calculated to as high a level of accuracy as the QCD predictions discussed below.

Perturbative QCD predictions for $\langle N_{\rm g}-1\rangle$ and $\langle N_{\rm q}-1\rangle$ were obtained in two different approximations [2]. (a) Calculations exact to leading order in α_s (referred to in the following as LO) are based on the $O(\alpha_s^2)$ matrix element, since one order of α_s is necessary to produce

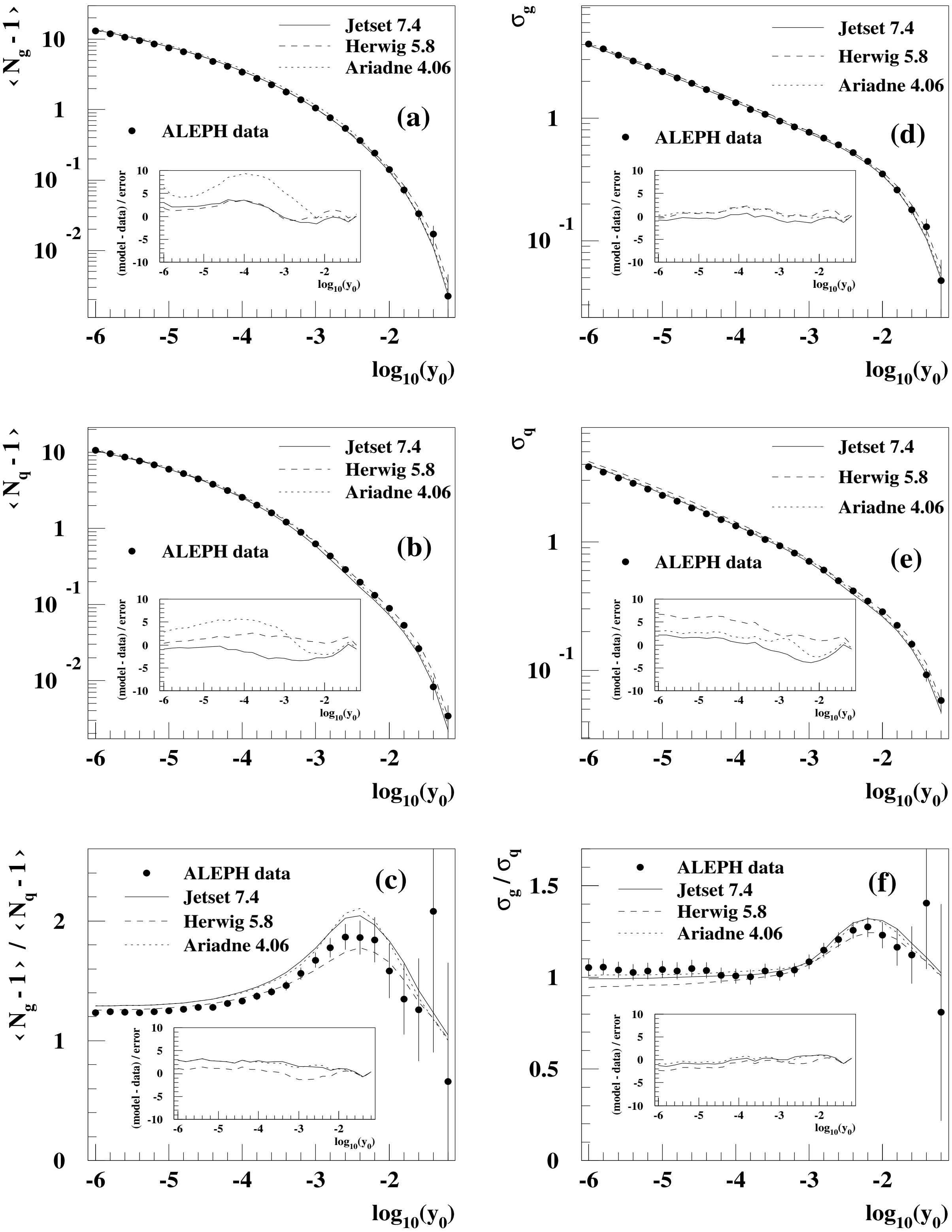

Figure 4: The mean (left-hand side) and the width (right-hand side) of the subjet multiplicity distribution are shown for gluon jets, quark jets and the ratio $\frac{gluon}{quark}$ as a function of the subjet resolution parameter y_0. The full dots show the measurement and the different lines represent the predictions of MC models. The inset plots show the deviations of the model predictions from the data divided by the total error. All plots apply to the whole interval of available jet energies.

PRELIMINARY

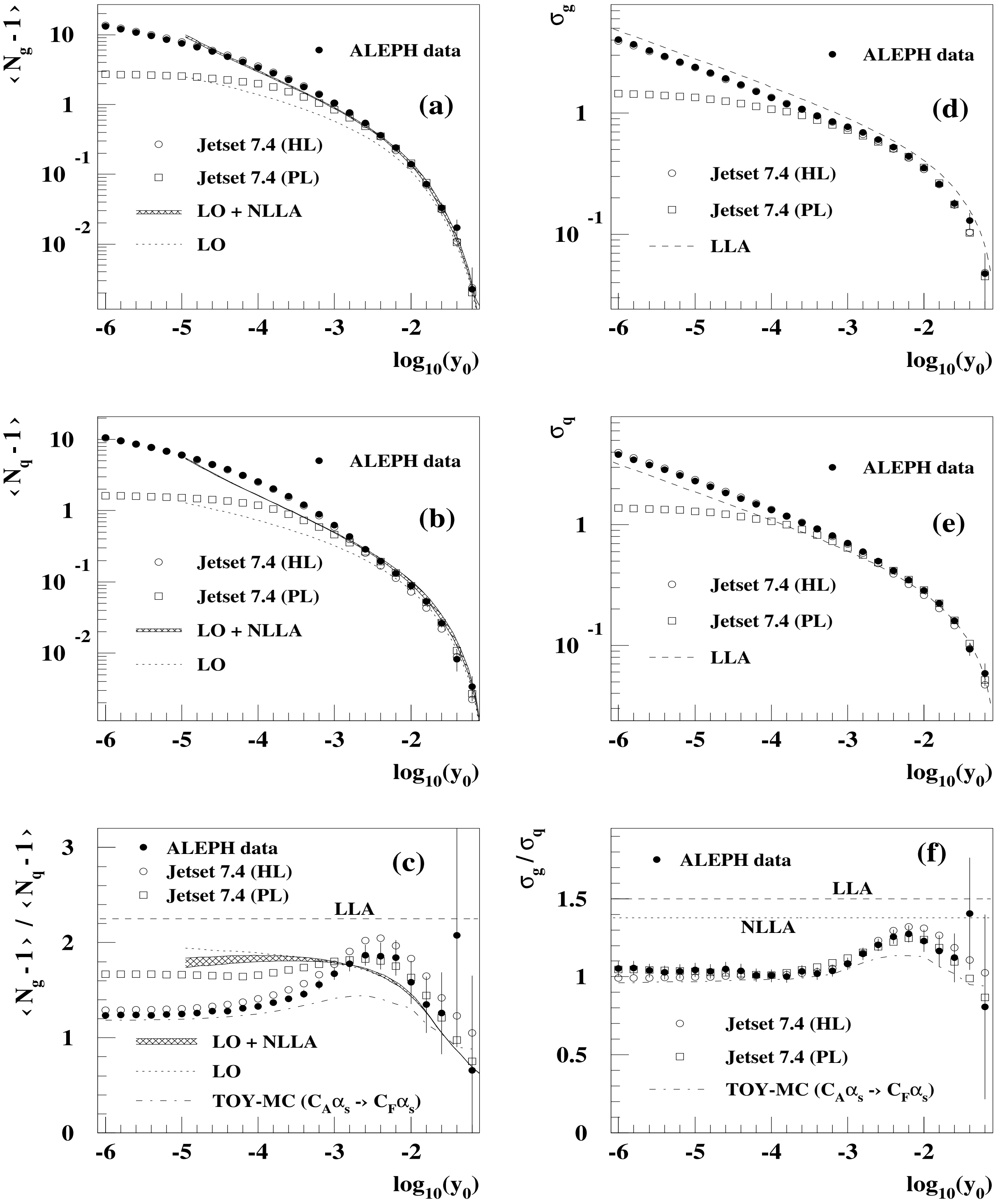

Figure 5: The mean (left-hand side) and the width (right-hand side) of the subjet multiplicity distribution are shown for gluon jets, quark jets and the ratio $\frac{gluon}{quark}$ as a function of the subjet resolution parameter y_0. The full dots show the measurement and the open circles and squares represent the hadron and parton level from the JETSET MC (if the open circles are not visible in some of the plots they lie on top of the data points). The dashed-dotted line in the ratio plots shows the hadron level prediction of a toy-MC (see Sect. 4.1). All the other lines show perturbative QCD predictions in different precision (see text).

a three-jet event. (b) By combining the LO result with the resummation of leading and next-to-leading logarithmic terms in y_1/y_0 to all orders in α_s, a much better approximation (referred to in the following as LO+NLLA) is obtained. From Figs. 5(a) and (b), one can see that the leading order prediction (LO) is compatible with the data only at very high values of y_0. A better description, extending to around $y_0 \approx 10^{-3}$ for both quark and gluon jets, is given by the parton level predictions of JETSET. Further improvement is obtained by the LO+NLLA prediction (shown in Figs. 5(a) – (c) as a hatched area between two lines): approximate agreement for gluon jets is extended down to $y_0 \approx 10^{-5}$, and to around 10^{-3} for quark jets. The earlier onset of the discrepancy for quark jets has been shown by Monte Carlo studies to result from the presence of quarks mass and hadronization effects. In fact these studies show that the fall-off of R_N at small y_0 is due partly to the higher multiplicity b-quark jets, which start to exert their influence for decreasing y_0 at around $y_0 \sim 10^{-2.6}$.

Resumming the logarithms of y_1/y_0 has roughly the same influence on both $\langle N_{\rm g} - 1\rangle$ and $\langle N_{\rm q} - 1\rangle$, so that this has little influence on R_N, i.e. the LO and LO + NLLA predictions for R_N are very similar. If only the leading-log contributions (LLA) are considered, the QCD prediction for the ratio R_N is given by the ratio of colour factors $R_N = C_A/C_F = 9/4$, independent of y_0. Including the fixed order (LO) calculation not only lowers the prediction, bringing it in closer agreement with the data, but also provides qualitatively the correct y_0 dependence for large y_0 (cf. Fig. 5(c)).

The plot of the ratio R_N in Fig. 5(c) also shows the hadron level prediction of the toy Monte Carlo where the effective coupling for the branching $g \to gg$ was changed from $C_A\alpha_s$ to $C_F\alpha_s$ (cf. Section 4.1). In the region where hadronization effects are expected to be small ($10^{-3} < y_0 < 10^{-2}$), the ratio R_N is around 1.3 – 1.4, whereas for the standard JETSET model it is predicted to rise to around 2. This indicates that one is sensitive to perturbatively predicted features. For smaller y_0, however, the standard and toy models give similar predictions, indicating that here R_N is not sensitive to the effective colour charge in the parton shower.

For the standard deviations, $\sigma_{\rm g}(y_0)$ and $\sigma_{\rm q}(y_0)$, the analytical prediction as a function of y_0 is only available in leading-log accuracy [13, 14]. The y_0 dependence for both quantities is the same, and hence the prediction for the ratio is a constant. This is given by the ratio of colour factors $R_\sigma = \sqrt{C_A/C_F} = 3/2$ [14]. For the ratio R_σ, the prediction in next-to-leading log approximation is also available [15]. In both leading and next-to-leading log accuracy, R_σ is predicted to be greater than one, i.e. gluon jets should have a broader multiplicity distribution than quark jets. Other QCD calculations [16], however, have led to predictions of R_σ less than one, which is in disagreement with the data in the perturbative region.

The standard deviations $\sigma_{\rm g}$ and $\sigma_{\rm q}$ are in qualitatively good agreement with the LLA prediction. The agreement may in fact be better than expected, since these quantities should be sensitive to next-to-next-to-leading logarithmic terms in y_1/y_0 [17]. Although the y_0 dependence of $\sigma_{\rm g}$ and $\sigma_{\rm q}$ are well reproduced, one can see that the overall normalization of the LLA curves is not correctly predicted. By changing the value of α_s one can obtain a better agreement with the data for gluon jets ($\alpha_s \approx 0.09$) or with the data for quark jets ($\alpha_s \approx 0.15$), but not simultaneously for both. This suggests that higher order corrections should primarily affect the relative normalization of the gluon and quark jet curves.

In fact, a next-to-leading log prediction is available for the ratio R_σ and this shows better agreement with the data than the LLA in the perturbative region near $y_0 \simeq 10^{-2}$ (see Fig. 5(f)). In principle, calculations based on resummation of logarithms of y_1/y_0 should be most reliable for small y_0 (i.e. large logarithms). In this limit, however, hadronization effects for $\sigma_{\rm g}$ and $\sigma_{\rm q}$ are large, and indeed one sees that the agreement with the data for R_σ is poor. The measured

R_σ at small y_0 is approximately 1, so that here no significant difference between quark and gluon jets is visible. In the perturbative region around $y_0 \simeq 10^{-2}$, the hadronization effects are relatively small and $\ln y_1/y_0 \approx 2$ to 3 is sufficiently large that the resummed prediction is valid. This discussion of the resummed prediction for R_σ is correspondingly valid for the ratio R_N.

The decrease of $R_N(y_0)$ and $R_\sigma(y_0)$ for $y_0 \to y_1$ seen in Figs. 4 and 5 can at least partly be explained by the difference in the mean gluon and quark jet energies. The mean gluon jet energy is measured to be around 14% lower than the mean quark jet energy. Since it is possible to resolve an additional subjet at the scale $y_0 \lesssim y_1$ only for very high energy jets, this is more likely to be the case for quark jets, and therefore the ratio R_N is suppressed. This effect can be explored further by measuring the properties of the subjet multiplicity distribution for jets in a specific bin of jet energy, as done in the next section.

4.3 Subjet structure as a function of jet energy

In this section, the properties of the subjet multiplicity distribution are examined for samples of jets having approximately the same energy. Figure 6, for example, shows the mean multiplicities, $\langle N_\mathrm{g} - 1\rangle$ and $\langle N_\mathrm{q} - 1\rangle$, the standard deviations, σ_g and σ_q, and their ratios, R_N and R_σ, for jets in the energy range $24\,\mathrm{GeV} \leq \mathrm{E_{jet}} \leq 28\,\mathrm{GeV}$. The dependence on y_0 is qualitatively similar to that of the energy-integrated case. There is also a similar level of agreement with the Monte Carlo models. Effects caused by the mean energy difference between quark and gluon jets, however, are now largely removed. This results in a larger rise in the ratios R_N and R_σ for y_0 in the perturbative region, and a less pronounced fall off for $y_0 \to y_1$ (compare Fig. 6(c) and 6(f) with Fig. 4(c) and Fig. 4(f)). When E_jet is restricted, preturbative QCD predictions are only available for the mean subjet multiplicities. A comparison of this with the data (not shown) leads to similar conclusions as those drawn in Section 4.2.

The dependence on y_0 in different jet energy bins can be understood by looking at the mean multiplicities and standard deviations as a function of E_jet for a fixed value of $y_0 = 10^{-2.2}$ (corresponding to a transverse momentum separation between subjets of $k_t = E_\mathrm{cm}\sqrt{y_0} \approx 7.2\,\mathrm{GeV}$), as shown in Fig. 7. The value of y_0 was chosen to be in the region where one is sensitive to perturbative effects and where hadronization effects are relatively small. From Fig. 7 one can see that the multiplicities and standard deviations increase as a function of E_jet. But if the ratios R_N and R_σ from the energy integrated jet samples are considered, one compares gluon jets with a mean of 26.2 GeV with quark jets having a mean energy of 30.4 GeV. Therefore, this results in a lower ratio than in the case where jets of equal energies are compared. Measurements at other y_0 values show a similar dependence on E_jet.

While $\langle N_\mathrm{g} - 1\rangle$ steadily increases with increasing jet energy, $\langle N_\mathrm{q} - 1\rangle$ first shows a gentle rise and then, from about $E_\mathrm{jet} = 40\,\mathrm{GeV}$ on, increases sharply (cf. Figs. 7(a) and (b)). As a result, R_N shows a clear E_jet dependence, first increasing, and then decreasing sharply to approximately 1.0 at $E_\mathrm{jet} \approx 40\,\mathrm{GeV}$. This behaviour can be explained by the fact that jets with very high energies often also have a high invariant mass; this is a consequence of four-momentum conservation for the three-jet event. The most probable way for this to occur is by means of a parton splitting (e.g. $g \to gg$ or $q \to qg$) which leads to a high mass parton pair; as a result the jet contains two clearly separated subjets. The mean multiplicity of such jets, for both quark and gluon, even at high subjet resolution parameters is around 2 and therefore the ratio R_N is about 1. Events with at least one jet of very high energy thus represent a special class; they would have been clustered to four-jet events if a slightly lower jet resolution parameter y_1 (< 0.1) had been used. This dependence on E_jet is well predicted by all of the Monte Carlo

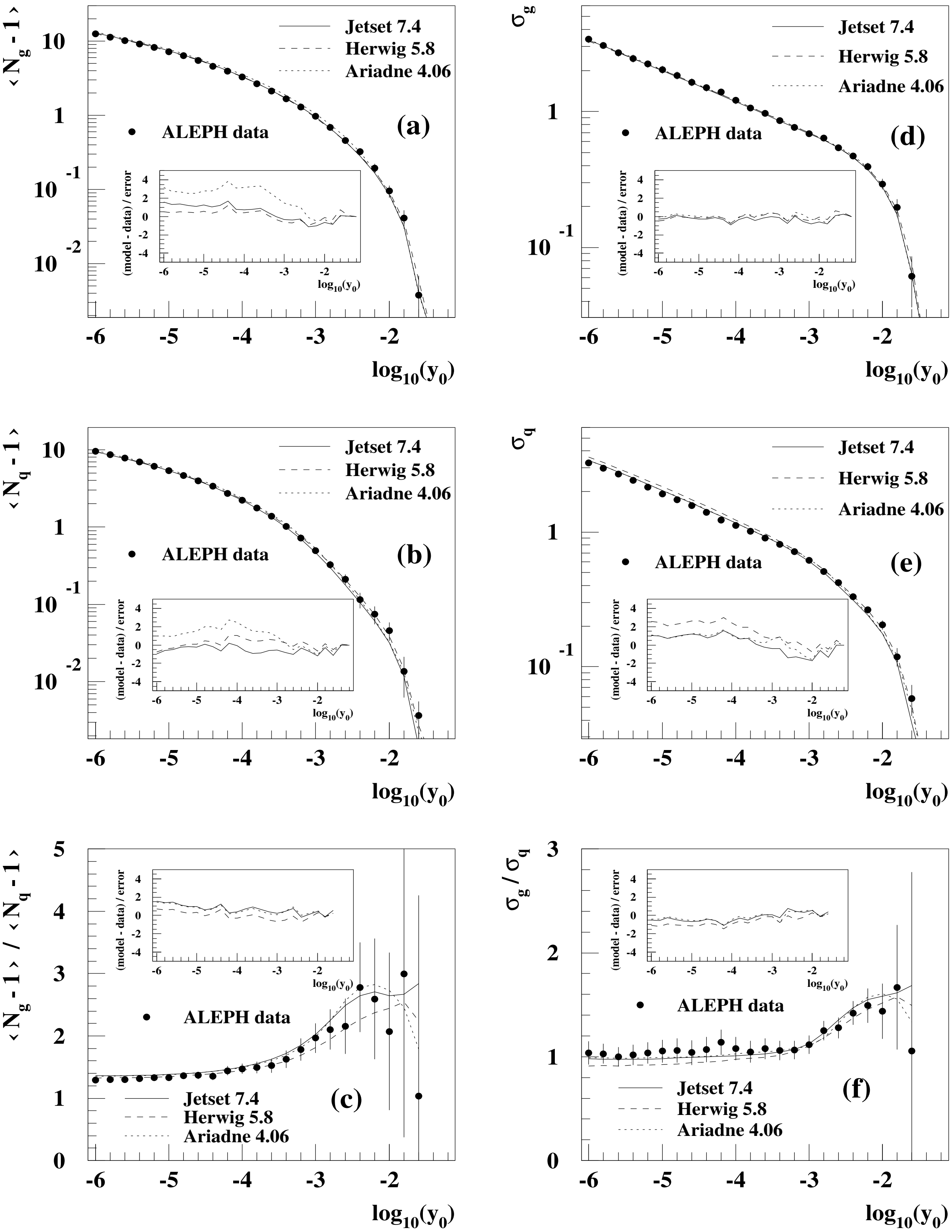

Figure 6: The mean (left-hand side) and the width (right-hand side) of the subjet multiplicity distribution for gluon and quark jets, as well as the corresponding ratios R_N and R_σ, for jets in the energy range $24\,\mathrm{GeV} \leq \mathrm{E_{jet}} \leq 28\,\mathrm{GeV}$. The points show the measurement and the lines are the predictions of Monte Carlo models. The inset plots show the deviations of the model predictions from the data divided by the total error.

PRELIMINARY

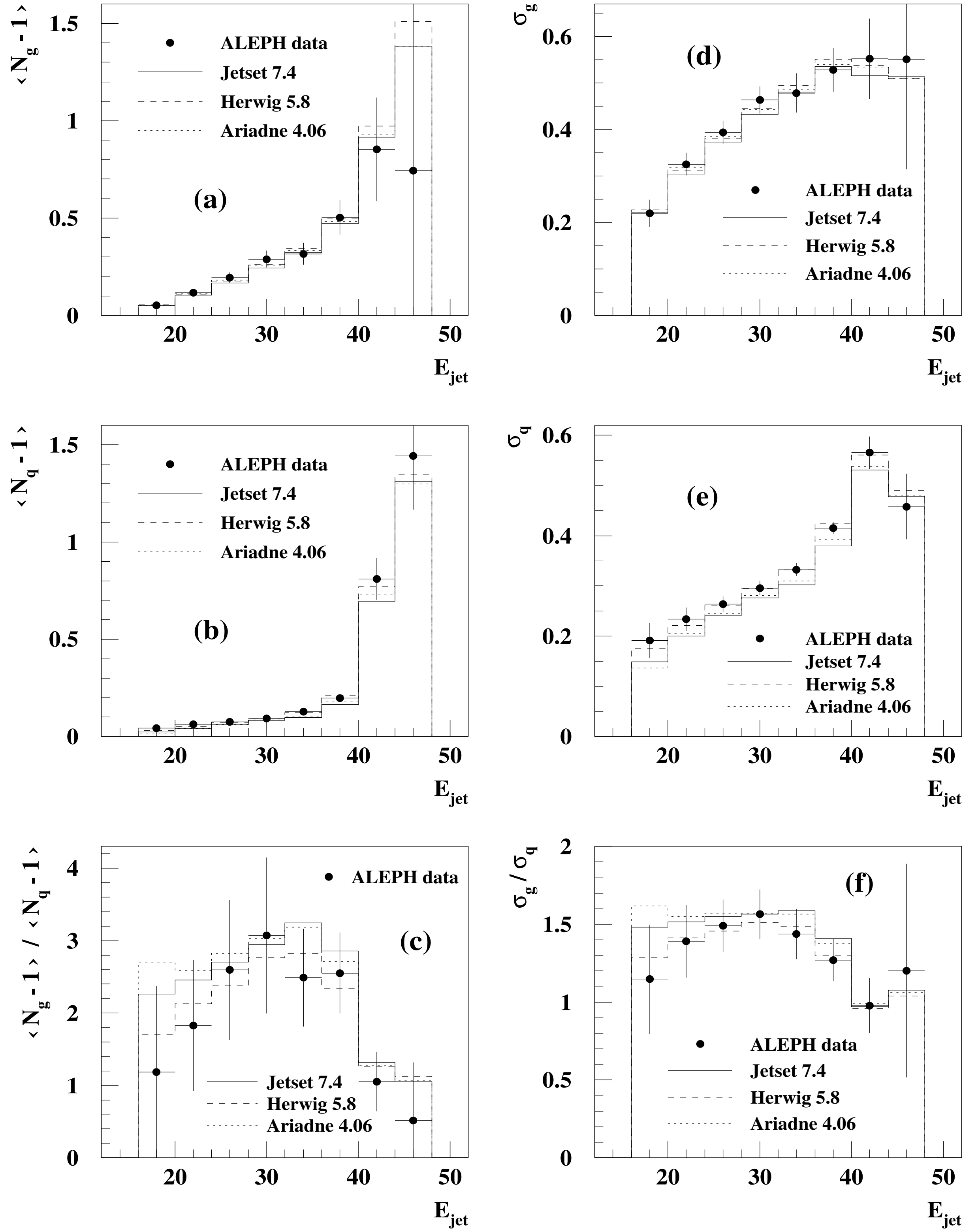

Figure 7: The mean (left-hand side) and the width (right-hand side) of the subjet multiplicity distribution for gluon and quark jets, as well as the ratios R_N and R_σ for fixed $y_0 = 10^{-2.2}$ as a function of $E_{\rm jet}$. The points show the measurement and the curves show the predictions of Monte Carlo models.

models considered.

Similar considerations also hold for the standard deviations $\sigma_{\rm q}$, $\sigma_{\rm g}$ and their ratio R_σ. In particular, R_σ is found to drop to around one for $E_{\rm jet} > 40$ GeV.

As noted above for the case 24 GeV $< E_{\rm jet} <$ 28 GeV, the agreement between data and perturbative QCD for $\langle N_{\rm g} - 1\rangle(y_0)$, $\langle N_{\rm q} - 1\rangle(y_0)$, and $R_N(y_0)$ is reasonable as $y_0 \to y_1$, although there the statistical errors are large. This statement is also true for other bins of jet energy up to around 40 GeV; for higher jet energies the perturbative prediction cannot describe the data. This is because the calculation is only of leading order in α_s, which describes a maximum of two hard resolvable partons per jet. Therefore, the invariant masses of the jets cannot on average be as high as in the real data and jet energies above 42 GeV are not accessible. The data and QCD prediction are nevertheless close in the energy integrated case, Figs. 5(a) – (c), because the very small number of jets with energies above 40 GeV carry little statistical weight.

4.4 Fragmentation function for charged particles

Figure 8 shows the measured inclusive distribution of $x = E_{\rm hadron}/E_{\rm jet}$ (the fragmentation function) for charged particles in quark and gluon jets selected here with $y_{\rm cut} = 0.1$ along with the predictions of Monte Carlo models. Here the jet energies were estimated from the angles between the three jets using the kinematic relation for massless jets. While all models describe the spectrum for quark jets quite well, the fragmentation function for gluon jets is predicted softer than measured. As has been observed before [18], this discrepancy is greatest for the HERWIG model.

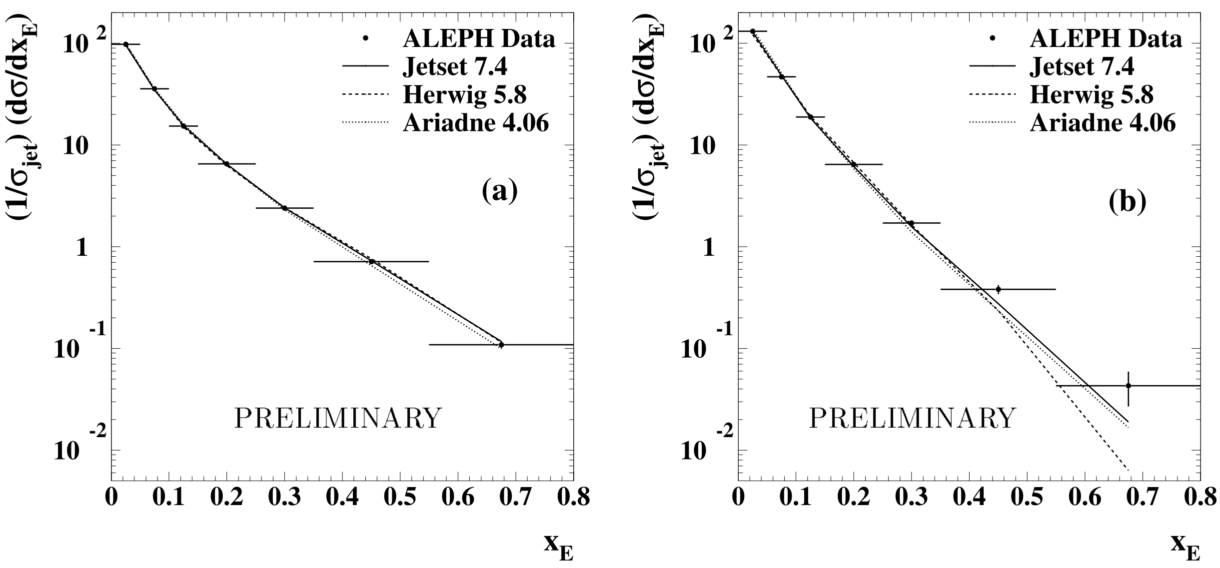

Figure 8: The measured fragmentation function for (a) quark and (b) gluon jets along with the predictions of Monte Carlo models.

Because the effective coupling for $g \to gg$ is larger than that of $q \to qg$, gluon jets are expected to have higher multiplicities and therefore a softer fragmentation function than quark jets. This is in fact observed. Although the exact forms of the fragmentation functions cannot be calculated using perturbative QCD, their energy dependence can be predicted by the DGLAP evolution equations [19]. The measured distributions presented here can be used as input for an investigation of this energy dependence (scaling violation) as was done, for example, in [20].

The measurements presented here are in agreement with the previous results from LEP experiments [18], which were typically based on jets selected with a resolution parameter of $y_{\rm cut} = 0.01 - 0.02$. This corresponds to an energy scale for the jets of $Q = \sqrt{y_{\rm cut}}E_{\rm cm} \approx 10$ GeV. In the present measurement, however, jets are selected with $y_{\rm cut} = 0.1$, so one probes for the first time the higher scale of $Q \approx 30$ GeV. Non-perturbative corrections to the fragmentation function are expected to fall as the energy scale increases. If the energy dependence is assumed to be $1/Q$ (see e.g. [21]), such effects are reduced by about a factor of three at the higher scale. In addition, the measurements here have significantly smaller uncertainties, owing mainly to the large data sample and high gluon jet purity. The measurements here thus provide a more reliable prediction for jets in the energy range to be probed at the Large Hadron Collider (10^2 – 10^3 GeV) than was previously available from e^+e^- data.

5 Summary and conclusions

70 000 symmetric three-jet events ($y_{\rm cut} = 0.1$ for the Durham algorithm) have been selected from $3 \cdot 10^6$ hadronic Z decays recorded by the ALEPH detector. From these events, a sample of 4 000 gluon jet candidates with a purity of $(94.4 \pm 0.3(\text{stat.}))\%$ have been identified by means of an impact parameter tagging method. With these data the properties of quark and gluon jets have been studied over a broad range of scales, covering hard and soft phenomena.

The jet broadening distribution and the differential one-subjet rate have been exploited to characterize the jet shape. These observables show a sensitivity to perturbative QCD at hard scales and are found to be compatible with the predictions of different Monte Carlo models.

In order to further resolve the substructure of jets, the subjet multiplicity distribution has been studied. By measuring the mean and the width of this distribution as a function of the subjet resolution scale, the transition from hard to soft QCD has been studied. These quantities are also sensitive to perturbative QCD and in general are also found to be compatible with the predictions of different MC generators. However, it was shown that the subjet multiplicity distribution for the quark jets predicted by HERWIG version 5.8 is significantly too broad, while the same quantity for gluon jets is in good agreement with the data. These observables were also compared with perturbative predictions, which show that leading and next-to-leading logarithmic terms are necessary in order to extent perturbative descriptions down to softer QCD scales. For quark jets the agreement is achieved down to $y_0 \approx 10^{-3}$, whereas the predictions for gluon jets describe the data down to scales of $y_0 \approx 10^{-5}$.

Finally, a precise measurement of the fragmentation function for charged particles in quark and gluon jets has been carried out using a hard QCD scale for the jet selection. This can serve as input for studies of scaling violations and can be used to predict the properties of gluon jets produced in other processes.

Acknowledgements

We would like to thank M.H. Seymour for many helpful discussions. His QCD predictions were an important motivation for doing many of the studies presented. We wish to thank our colleagues from the accelerator divisions for the successful operation of LEP. It is also a pleasure to thank the technical personnel of the collaborating institutions for their support in constructing and maintaining the ALEPH experiment. Those of the collaboration not from member states thank CERN for its hospitality.

References

[1] ALEPH Collaboration, D. Buskulic et al., *Phys. Lett.* **B 346** (1995) 389.

[2] M.H. Seymour, *Phys. Lett.* **B 378** (1996) 279.

[3] S. Catani and M. H. Seymour, private communication.

[4] ALEPH Collaboration, D. Decamp et al., *Nucl. Instr. Meth.* **A 294** (1990) 121.

[5] W.J. Stirling, J. Phys. **G** *Nucl. Part. Phys.* **17** (1991) 1567.

[6] S. Catani, G. Turnock and B. R. Webber, *Phys. Lett.* **B295** (1992) 269.

[7] ALEPH Collaboration, D. Decamp et al., *Phys. Lett.* **B 313** (1993) 535.

[8] T. Sjöstrand, *Comp. Phys. Comm.* **82** (1994) 74.

[9] G. Marchesini et al., *Comp. Phys. Comm.* **67** (1992) 465.

[10] L. Lönnblad, *Comp. Phys. Comm.* **71** (1992) 15.

[11] ALEPH Collaboration, R. Barate et al., *Studies of Quantum Chromodynamics with the ALEPH Detector*, CERN-PPE/96-186.

[12] ALEPH Collaboration, D. Buskulic et al., *Z. Phys.* **C 69** (1995) 15.

[13] M.H. Seymour, private communication.

[14] A. Bassetto, M. Ciafaloni, G. Marchesini, *Nucl. Phys.* **B 163** (1980) 477.

[15] E.D. Malaza and B.R. Webber, *Phys. Lett.* **B 149** (1984) 501.

[16] I.M. Dremin, *Physics-Uspekhi* **37**(8) (1994) 715.

[17] Yu.L. Dokshitzer, *Phys. Lett.* **B 305** (1993) 295.

[18] OPAL Collaboration, *Z. Phys.* **C68** (1995) 179;
DELPHI Collaboration, *EPS-HEP 95* Ref. eps0547;
ALEPH Collaboration, *Phys. Lett.* **B 384** (1996) 353.

[19] V.N. Gribov und L.N. Lipatov, *Sov. J. Nucl. Phys.* **15** (1972) 78;
G. Altarelli und G. Parisi, *Nucl. Phys.* **B 126** (1977) 298;
Yu.L. Dokshitzer, *Sov. Phys. JETP* **46** (1977) 641.

[20] ALEPH Collaboration, D. Buskulic et al., *Phys. Lett.* **B 357** (1995) 487.

[21] P. Nason and B.R. Webber, *Nuclear Physics* **B 421** (1994) 473.